

Photophysics of 2'-Deoxyuridine (dU) Nucleosides Covalently Substituted with Either 1-Pyrenyl or 1-Pyrenoyl: Observation of Pyrene-to-Nucleoside Charge-Transfer Emission in 5-(1-Pyrenyl)-dU

Thomas L. Netzel,^{*,†,§} Min Zhao,[§] Kambiz Nafisi,[§] Jeb Headrick,[‡] Matthew S. Sigman,^{‡,⊥} and Bruce E. Eaton^{*,⊥}

Contribution from the Department of Chemistry, Georgia State University, Atlanta, Georgia 30303, and Department of Chemistry, Washington State University, Pullman, Washington 99164-4630

Received January 23, 1995[⊗]

Abstract: This paper reports syntheses, electronic absorbance and emission spectra, and emission kinetics results for two types of pyrene-substituted uridine nucleosides as part of an ongoing study which is examining the photophysical and photochemical behaviors of these same nucleosides embedded in DNA oligomers and duplexes with varying base-sequence composition. The two labels are 1-pyrenyl itself and 1-carboxypyrenyl (1-pyrenoyl) which are each joined directly to the 5-position of 2'-deoxyuridine (dU). These direct attachments significantly restrict the range of conformations available to the pyrene label when it is attached to a DNA oligomer or duplex. π, π^* emission is absent for 5-(1-pyrenyl)-dU, **1**, in methanol (MeOH) but present in tetrahydrofuran (THF). For **1** in MeOH, broad charge-transfer (CT) emission is present with a maximum at 470 nm and a quantum yield of 0.027; for **1** in THF, π, π^* emission is present with a maximum at 395 nm and quantum yield of 0.42. Thermodynamic considerations suggest that the CT photoproduct of **1** which emits in MeOH is pyrene⁺/dU⁻. The emission kinetics of **1** in MeOH are triexponential, but the wavelength variation of the relative amplitudes of the different decay lifetimes indicates that the CT-state relaxations are biexponential with lifetimes of ≤ 50 ps and 0.9 ns. Similarly, the π, π^* state of **1** in MeOH also has two electron transfer (ET) quenching lifetimes of ≤ 50 ps and 2–3 ns. The steady-state emission spectrum of **1** in MeOH shows that emission from the few long-lived π, π^* states is dominated at all wavelengths by the 0.9-ns lived CT emission. In contrast, only π, π^* emission is observed for 5-(1-pyrenoyl)-dU, **2**, in both MeOH and THF with emission quantum yields of 0.002 and 0.028, respectively. The emission kinetics for **2** in THF are at least quadruply exponential having the longest emission lifetime of *ca.* 95 ns. However, only about 10% of the relative emission amplitude decays with lifetimes greater than 10 ns. Approximately 90% of the emission amplitude decays on the same time scale as for **2** in MeOH. The spectral and emission kinetics data for nucleosides **1** and **2** support the conclusions that each has multiple conformers in solution and that the relative orientation of the pyrene and uridine π -systems plays a crucial role in determining the rates of both ET quenching of pyrene* and charge-recombination in the photoproduct.

Introduction

In this paper we lay the groundwork for studying ET reactions within DNA duplexes by examining the photophysics of uridine nucleosides which are covalently labeled at the 5-position with 1-pyrenyl chromophores. Pyrenyluridine analogs with well defined direct attachment to the 5-position of uridine had not been reported previously requiring the development of the synthetic methodology reported herein. Previous methods to prepare **1** resulted in a mixture of pyrene regioisomers,¹ which were not suitable for our photophysical studies. Photoredox-active labels attached directly to uridine are most desirable because they have a limited number of conformations making both NMR and molecular modeling studies more tractable.^{2,3}

There are few published studies of covalently substituted bases in well-defined nucleic acid environments. In contrast,

there are many studies of the photophysical properties of polyaromatic hydrocarbon (PAH)/DNA and other chromophore/nucleic acid complexes. However, these latter studies are of systems which contain a large number of chromophore micro-environments and thus are difficult to interpret without ambiguity. This work begins to establish the photophysical and photochemical properties of some well-defined chromophore/nucleic acid complexes.

Pyrene–uridine conjugates have been used previously because pyrene is a stable chromophore with a reasonably long fluorescence lifetime (*ca.* 200–400 ns) depending upon the type of substitution and solvent.^{4–7} Its long emission lifetime is a consequence of the fact that π, π^* absorption to its lowest-energy electronic excited state (S_1) is spin-allowed but orbitally forbidden.^{8,9} Since it is conveniently derivatized at the 1-position, it has frequently been employed as a fluorescent label

[†] (Phone) 404-651-3129; FAX 404-651-1416.

[‡] Present address: NeXstar Pharmaceuticals, Boulder, CO 80301.

[§] Georgia State University.

[⊥] Washington State University.

[⊗] Abstract published in *Advance ACS Abstracts*, August 15, 1995.

(1) Saito, I.; Ito, S.; Shinmura, T.; Matsuura, T. *Tetrahedron Lett.* **1980**, *21*, 2813.

(2) Veal, J. M.; Wilson, W. D. *J. Biomol. Struct. Dyn.* **1991**, *8*, 1119.

(3) Kollman, P. in *Protein Des. Dev. New Ther. Vaccines*; Hook, J. B., Poste, G., Eds.; Plenum: New York, NY, 1990; p 229.

(4) Cundall, R. B. *Photochemistry* **1992**, *23*, 3.

(5) Ahuja, R. C.; Moebius, D. *Langmuir* **1992**, *8*, 1136.

(6) Kalyanasundaram, K.; Thomas, J. K. *J. Am. Chem. Soc.* **1977**, *99*, 2039.

(7) Lianos, P.; Cremel, G. *Photochem. Photobiol.* **1980**, *31*, 429.

(8) Lianos, P. C. *Photophysical Properties of Pyrene of Biophysical Importance*; Univ. Tennessee, Knoxville, TN, USA, p 158. Avail. Univ. Microfilms Int., Order No. 7903440 From: *Diss. Abstr. Int. B* **1979**, *1978*, 39(8), 3656.

especially in biological studies.^{5,7,10-18} It is also true that pyrene can be reversibly oxidized and reduced in both its ground and lowest-energy excited states.¹⁹⁻²⁴ Recently its photophysics has been extensively studied as a carcinogenic and mutagenic benzo-[a]pyrenediol epoxide (BPDE) derivative bound to the exocyclic amino group of guanosine (dG) nucleosides in native DNA.^{12,13,16,20,25,26} In polar organic solvents dG quenches the emission of photoexcited BPDE and yields pyrenyl radical anions. However, in the same solvents the covalent adduct of BPDE and dG does not show radical products on time scales greater than 10 ns, but it does show enhanced triplet formation mostly likely due to intramolecular ET excited-state quenching followed by rapid back ET. A recent picosecond kinetics study was the first to provide unambiguous evidence of ET between photoexcited pyrene (pyrene*) and a covalently attached nucleic acid base.²³ However, in general it is possible for other processes to be important in the excited state deactivation of pyrene* by nucleic acid bases.

From a different vantage point, studies of radiation damage in biological systems are concerned with the identity of products of DNA oxidation and reduction, their rates of formation and decay, and their states of protonation.²⁷⁻³⁶ While numerous studies of DNA bases, nucleosides, and monophosphate nucleotides have been conducted, it is generally difficult to investigate

oxidation and reduction processes in DNA oligomers and duplexes at specific base sites.

The above characteristics imply that following photoexcitation pyrene* can directly inject an electron into uridine. The fate of the reduced uracil radical anion in both oligomers and duplexes with a variety of nearest neighbor bases may therefore be able to be examined. In related work we have shown that cytidine nucleotides are better ET quenchers of pyrene* emission than are thymidine nucleotides.³⁷ This nucleoside reactivity ranking supports conclusions drawn from γ -irradiation studies of DNA.³⁸ In this latter work, initially formed $dT^{\cdot-}$ was shown upon warming to form the reversibly protonated ET product, $dC(N3)H^{\cdot}$. These results imply that it is possible for a reduced uridine (or thymidine) to transfer an electron to a nearby cytidine nucleotide. How effectively such secondary, internucleotide ET can compete in oligomers or in duplexes with charge recombination within a covalently labeled uridine nucleoside is a significant question.³⁹⁻⁴⁵

For the study reported in this paper two nucleosides were prepared, 5-(1-pyrenyl)-2'-deoxyuridine (1) and 5-(1-carboxypyrenyl)-2'-deoxyuridine (2), which have only one and two rotatable bonds, respectively, between the base and the label. These uridine analogs are suitable for transformation into phosphoramidite reagents and for incorporation into single and double strand oligonucleotides.⁴⁶ Pyrene was chosen as a label for uridine in this work because (1) it can have a long-lived singlet excited state, (2) it is a reversible electron donor and acceptor in its ground and excited states, and (3) ET from pyrene to uridine is estimated (see below) to be very exergonic for pyrene's S_1 state (pyrene*). The goals of the study reported here are (1) to elucidate the photophysics of pyrene/uridine nucleoside adducts and (2) to establish a foundation for subsequent investigations of pyrene/uridine adducts in DNA oligomers and duplexes. These latter studies are of interest from at least three different perspectives. First, there is interest in understanding and controlling ET dynamics among DNA bases and DNA adducts in oligomers and duplexes.^{39,43,45,47-51} Second, knowledge of the rates of DNA base ionizations and neutralizations is useful in unraveling the mechanisms of DNA damage caused by ionizing radiation.^{36,52-56} Third, pyrene—

(9) Turro, N. J. *Modern Molecular Photochemistry*; Benjamin/Cummings Publishing Co., Inc.: Menlo Park, CA, 1978.

(10) Lianos, P.; Duportail, G. *Eur. Biophys. J.* **1992**, *21*, 29.

(11) Duportail, G.; Lianos, P. *Chem. Phys. Lett.* **1990**, *165*, 35.

(12) Eriksson, M.; Kim, S. K.; Sen, S.; Graslund, A.; Jernstrom, B.; Norden, B. *J. Am. Chem. Soc.* **1993**, *115*, 1639.

(13) Geacintov, N.; Prusik, T.; Khosrofiyan, J. *J. Am. Chem. Soc.* **1976**, *98*, 6444.

(14) Graslund, A.; Kim, S. K.; Eriksson, S.; Norden, B.; Jernstrom, B. *Biophys. Chem.* **1992**, *44*, 21.

(15) Kano, K.; Matsumoto, H.; Hashimoto, S.; Sisido, M.; Imanishi, Y. *J. Am. Chem. Soc.* **1985**, *107*, 6117.

(16) Weston, A.; Bowman, E. D. *Carcinogenesis* **1991**, *12*, 1445.

(17) Telser, J.; Cruickshank, K. A.; Morrison, L. E.; Netzel, T. L. *J. Am. Chem. Soc.* **1989**, *111*, 6966.

(18) Telser, J.; Cruickshank, K. A.; Morrison, L. E.; Chan, C.-K.; Netzel, T. L. *J. Am. Chem. Soc.* **1989**, *111*, 7226.

(19) Kubota, T.; Kano, J.; Uno, B.; Konse, T. *Bull. Chem. Soc. Jpn.* **1987**, *60*, 3865.

(20) Shafirovich, R. Y.; Levin, P. P.; Kuzmin, V. A.; Thorgeirsson, T. E.; Klinger, D. S.; Geacintov, N. E. *J. Am. Chem. Soc.* **1994**, *116*, 63.

(21) Shida, T. *Electronic Absorption Spectra of Radical Ions*; Elsevier: New York, 1988.

(22) Weinstein, Y. A.; Sadovskii, N. A.; Kuz'min, M. G. *High Energ. Chem.* **1994**, *28*, 211.

(23) O'Connor, D.; Shafirovich, V. Y.; Geacintov, N. *J. Phys. Chem.* **1994**, *98*, 9831.

(24) Pysh, E. S.; Yang, N. G. *J. Am. Chem. Soc.* **1963**, *85*, 2124.

(25) Geacintov, N. E.; Zhao, R.; Kuzmin, V. A.; Seog, K. K.; Pecora, L. J. *Photochem. Photobiol.* **1993**, *58*, 185.

(26) Vahakangas, K.; Yrjanheikki, E. *IARC Sci. Publ.* **1990**, *104*, 199.

(27) Anderson, R. F.; Patel, K. B.; Wilson, W. R. *J. Chem. Soc., Faraday Trans.* **1991**, *87*, 3739.

(28) Bernhard, W. A. *NATO ASI Ser., Ser. H* **1992**, *54*, 141.

(29) Cadet, J.; Berger, M.; Mouret, J. F.; Odin, F.; Polverelli, M.; Ravanat, J. L. *NATO ASI Ser., Ser. H* **1992**, *54*, 403.

(30) Candeias, L. P. *Radiation chemistry of purines in aqueous solution*; Inst. Super. Tec., Tech. Univ. Lisbon, Lisbon, Port.: Report Order No. PB92-229418, 174 pp. (Port.) Avail. NTIS From Gov. Rep. Announce. Index (U.S.) **1992**, 92(23), Abstr. No. 265,515, 1992.

(31) Janovic, S. V.; Simic, M. *Biochim. Biophys. Acta* **1989**, *1008*, 39.

(32) Kittler, L.; Lober, G.; Gollmick, F.; Berg, H. *J. Electroanal. Chem.* **1980**, *116*, 503.

(33) Lin, N. *Res. Chem. Intermed.* **1990**, *14*, 209.

(34) Mark, F.; Becker, U.; Herak, J. N.; Schulte-Frohlinde, D. *Radiat. Environ. Biophys.* **1989**, *28*, 81.

(35) Schulte-Frohlinde, D.; Bothe, E. *NATO ASI Ser., Ser. H* **1991**, *54*, 317.

(36) Sevilla, M. D. *Mechanisms for Radiation Damage in DNA. Comprehensive Report, June 1, 1986-May 31, 1992*; U. S. Department of Energy, Division of Energy Research: INIS 23:29887 DOE/ER/60455-6, 1991.

(37) Manoharan, M.; Tivel, K.; Zhao, M.; Nafisi, K.; Netzel, T. L. *J. Phys. Chem.* In press.

(38) Wang, W.; Sevilla, M. D. *Radiat. Res.* **1994**, *138*, 9.

(39) Lecomte, J. P.; Kirsch-De Mesmaeker, A.; Kelly, J. M.; Tossi, A. B.; Goerner, H. *Photochem. Photobiol.* **1992**, *55*, 681.

(40) Candeias, L. P.; Wolf, P.; O'Neill, P.; Steenken, S. *J. Phys. Chem.* **1992**, *96*, 10302.

(41) Steenken, S. *Free Radical Res. Commun.* **1992**, *16*, 349.

(42) Turro, N. J.; Barton, J. K.; Tomalia, D. In *Photochem. Convers. Storage Sol. Energy, Proc. Int. Conf., 8th, Meeting Date 1990*; Pelizzetti, E., Schiavello, M., Eds., Kluwer: Dordrecht, Netherlands, 1991; p 121.

(43) Risser, S. M.; Beratan, D. N.; Meade, T. J. *J. Am. Chem. Soc.* **1993**, *115*, 2508.

(44) Murphy, C. J.; Arkin, M. R.; Jenkins, Y.; Ghatlia, N. D.; Bossmann, S. H.; Turro, N. J.; Barton, J. K. *Science* **1993**, *262*, 1025.

(45) Brun, A. M.; Harriman, A. *J. Am. Chem. Soc.* **1994**, *116*, 10383.

(46) Eaton, B. E.; Headrick, J.; Sigman, M. S.; Netzel, T. L. (unpublished results).

(47) Purugganan, M. D.; Kumar, C. V.; Turro, N. J.; Barton, J. K. *Science* **1988**, *241*, 1645.

(48) Geacintov, N. E.; Mao, B.; France, L. L.; Zhao, R.; Chen, J.; Liu, T. M.; Ya, N. Q.; Margulis, L. A.; Sutherland, J. C. *Proc. SPIE Int. Soc. Opt. Eng.* **1992**, *1640*, 774.

(49) Takenaka, S.; Ihara, T.; Takagi, M. *Chem. Lett.* **1992**, *1*.

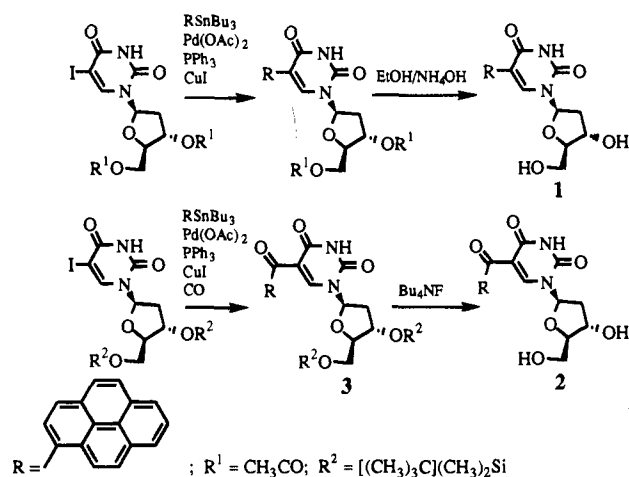
(50) Orellana, G.; Kirsch-De Mesmaeker, A.; Barton, J. K.; Turro, N. J. *Photochem. Photobiol.* **1991**, *54*, 499.

(51) Fox, M. A. In *Photoinduced Electron Transfer III*; Mattay, J., Eds.; Springer-Verlag: Berlin, Heidelberg, 1991; p 257.

(52) Symons, M. C. R. *NATO ASI Ser., Ser. H* **1992**, *54*, 111.

(53) Fielden, E.; O'Neill, P.; eds. *The Early Effects of Radiation on DNA*; NATO ASI Series H: Cell Biology, *54*, Springer-Verlag: Berlin, 1991; p 448.

Scheme 1



adduct lesions in DNA strands can be inserted into cellular hosts as sites of genetic mutations and thus are useful as tools for learning about DNA repair and replication mechanisms.

Materials and Methods

Synthesis, Purification, and Characterization. Assembly of the uridine analogs was accomplished by modification of previously published procedures.^{57,58} All palladium coupling reactions (Scheme 1) were conducted in a pressure-equalizing glass coupling apparatus equipped with an addition funnel and high vacuum Teflon valves. The starting reagents were combined in a Vacuum Atmospheres Inc. inert (argon) glovebox. Reactions conducted outside the glovebox were performed under an argon atmosphere. THF was distilled from benzophenone Na/K alloy. S/P Brand 60 A (230–400 mesh ASTM) silica was used for flash chromatography. NMR data were acquired on a Bruker AMX (300 MHz ¹H). Infrared data were acquired on a Perkin Elmer 1600 FTIR. Mass spectral data were obtained from the departmental facilities at Washington State University and the University of California at Berkeley.

5-(1-Pyrenyl)-2'-deoxyuridine (1). 3',5'-Bis(Acetyl)-5-iodo-2'-deoxyuridine (520 mg, 1.28 mmol), Pd(OAc)₂ (29.0 mg, 0.128 mmol), CuI (73 mg, 0.384 mmol), P(C₆H₅)₃ (101 mg, 0.384 mmol), and THF (15 mL) were combined in the coupling apparatus, the valves sealed and the coupling apparatus removed from the glovebox. A previously prepared solution of pyrenyl(tributyl)stannane (4) (755 mg, 1.54 mmol, in 10 mL of THF) was transferred into the reaction portion of the coupling apparatus via a cannula and the mixture heated to 70 °C. After 120 h at 70 °C, the solvent was removed on a rotary evaporator. The crude product was taken up in CH₂Cl₂ (5 × 1.5 mL portions) and applied to a pad of silica gel (65 g) in a glass-fritted Buchner funnel (150 mL). The solvent was eluted with pentane (150 mL), followed by CH₂Cl₂ (200 mL). The product was eluted with ethyl acetate (EtOH, 250 mL). The EtOH solution was concentrated on a rotary evaporator and the resulting residue purified by flash chromatography (200 g silica gel, EtOAc/petroleum ether/hexane, 55:30:15). The product was further purified by crystallization with a 5:3.5 mixture of EtOAc/hexane to yield 5-(1-pyrenyl)-2'-deoxyuridine as a light yellow solid (295 mg, 48%). Deprotection of 3',5'-bis(acetyl)-5-pyrenyl-2'-deoxyuridine was carried out by treatment with ethanolic ammonia (6 mL of ethanol, 6 mL of 12 M NH₄OH) at 55 °C for 12 h. The solution was evaporated on a vacuum line and the residue triturated with H₂O to give **1** (188 mg 41%) as a pale yellow solid: UV max (CH₃OH) 342 (ε 25,800) nm; ¹H NMR (300 MHz CD₃OD) δ 8.18 (m, 9H), 6.48 (t, *J* = 6.7 Hz, 1H) 4.43 (ddd, *J* = 8.3, 4.9, 3.5 Hz, 1H), 3.97 (q, *J* = 3.2 Hz, 1H),

3.71 (dd, *J* = 11.8, 3.0 Hz, 1H), 3.63 (dd, *J* = 12.0, 3.4 Hz), 2.43 (m, 2H); ¹³C{¹H} (75 MHz CD₃OD) δ 170.59, 170.38, 169.86, 162.15, 150.18, 145.17, 143.63, 138.88, 131.59, 131.16, 130.68, 128.11, 128.05, 127.18, 126.18, 125.57, 125.38, 124.60, 124.51, 117.43, 84.98, 82.27, 74.05, 63.87, 37.94; MS *m/z* 428.

5-(1-Pyrenyl)-2'-deoxyuridine (2). 3',5'-Bis(*tert*-butyldimethylsilyl)-5-(1-pyrenyl)-2'-deoxyuridine (**3**) (150 mg, 2.19 mmol), THF (5 mL), and Bu₄NF (4.82 mL of a 1 M solution in THF) were combined in a flask at room temperature. After stirring at room temperature for 1 h the reaction was treated with glacial acetic acid (270 μL) and the solution was concentrated on a rotary evaporator. Purification by anion exchange chromatography (80 g Duolite c-433 cation resin, H₂O/methanol, 75:25) and lyophilization of the product containing fractions gave **2** (91 mg, 91%) as a pale yellow solid: UV max (CH₃OH) 341 (ε 6950) nm; ¹H NMR (300 MHz CD₃OD) δ 8.49 (d, *J* = 9.3 Hz, 1H), 8.33 (m, 8H), 6.27 (t, *J* = 6.4 Hz, 1H), 4.26 (ddd, *J* = 9.3, 6.3, 3.4 Hz, 1H), 3.87 (q, *J* = 3.40 Hz, 1H), 3.36 (m, 2H), 2.42 (ddd, *J* = 13.5, 6.2, 3.4 Hz, 1H), 2.2 (dt, *J* = 13.5, 6.4 Hz, 1H); ¹³C{¹H} (100 MHz CD₃OD) δ 194.44, 162.69, 151.31, 150.27, 134.71, 134.46, 132.48, 131.91, 130.61, 130.23, 130.02, 128.24, 128.06, 127.49, 127.22, 126.96, 125.82, 125.45, 125.41, 125.05, 115.24, 89.40, 87.87, 72.21, 62.44, 41.97; HRMS (M + H) *m/z* for C₂₆H₂₁N₂O₆, calcd 457.1400, found 457.1402.

3',5'-bis(*tert*-butyldimethylsilyl)-5-(1-pyrenyl)-2'-deoxyuridine (3). 3',5'-Bis(*tert*-butyldimethylsilyl)-5-iodo-2'-deoxyuridine (1.00 g, 1.72 mmol), Pd(OAc)₂ (39 mg, 0.172 mmol), CuI (98 mg, 0.515 mmol), P(C₆H₅)₃ (135 mg, 0.515 mmol), and THF (18 mL) were combined in the coupling apparatus. A solution of pyrenyl(tributyl)stannane (**4**) (1.08 g, 2.06 mmol, in 7 mL of THF) was transferred into the reaction flask via cannula, and the apparatus was charged to 40 psi with CO and then heated to 70 °C. After stirring 48 h at 70 °C the solvent was removed on a rotary evaporator, and the crude product was filtered through a pad of silica gel as described for compound **1**. The resulting product was purified by flash chromatography (260 g silica gel, hexane/EtOAc, 60:40) to give **3** (1.07 g, 82%) as a pale yellow solid: UV max (CH₃OH) 341 (ε 6850) nm; ¹H NMR (300 MHz CD₃OD) δ 8.57 (d, *J* = 9.0 Hz, 1H), 8.26–8.02 (m, 8H), 6.32 (dd, *J* = 7.8, 5.7 Hz, 1H), 4.41 (dt, *J* = 4.2, 3.0 Hz, 1H), 4.04 (dt, *J* = 5.4, 3.0 Hz, 1H), 3.75 (dd, *J* = 11.4, 4.2 Hz, 1H), 3.68 (dd, *J* = 11.0, 4.2 Hz, 1H), 2.46 (ddd, *J* = 13.0, 5.7, 3.0 Hz, 1H) 2.13 (ddd, *J* = 13.0, 5.4, 7.8 Hz, 1H), 0.90 (s, 9H), 0.80 (s, 9H), 0.10 (s, 3H), 0.08 (s, 3H), 0.01 (s, 3H), -0.09 (s, 3H); ¹³C{¹H} (100 MHz CDCl₃) δ 191.66, 159.73, 149.53, 146.86, 133.66, 132.88, 131.18, 130.73, 129.60, 129.34, 127.33, 126.86, 126.32, 126.19, 125.99, 124.94, 124.56, 124.53, 123.83, 115.02, 88.84, 86.82, 77.32, 72.85, 63.12, 42.02, 25.94, 25.83, 18.38, 18.09, -4.60, -4.75, -5.46, -5.62. HRMS *m/z* for C₃₈H₄₈N₂O₆Si₂, calcd 684.3051, found 684.3007.

Pyrenyl(tributyl)stannane (4). 1-Bromopyrene (1.02 g, 3.61 mmol) and THF (20 mL) were placed in a flask and cooled to -78 °C. *tert*-butyllithium (4.25 mL, 7.22 mmol, of a 1.7 M solution) was added dropwise to the solution via a gas-tight syringe. After approximately 4 h at -78 °C the solution changed from its initial red color to yellow and a solution of Bu₃SnCl (980 μL, 3.61 mmol, in 15 mL of THF) was added via cannula. This mixture was allowed to warm to room temperature over a 2 h period then quenched with H₂O (1 mL). After an additional 8 h at room temperature the solvent was removed and the resulting viscous oil subjected to an aqueous workup. ¹H NMR analysis showed that no further purification was required and **4** was obtained as a viscous oil (1.74 g, 98%): UV max (CH₃OH) 244 (ε 15 015), 280 (ε 10 609) 332 (ε 8692) 348 (ε 11 630) nm; (300 MHz CDCl₃) δ ¹H NMR δ 8.21–7.87 (m, 9H), 1.73 (pent, *J* = 7.3 Hz, 6H), 1.46 (pent, *J* = 7.3 Hz, 6H), 1.41 (t, *J* = 7.3 Hz, 6H), 0.98 (t, *J* = 7.3 Hz, 9H); ¹³C{¹H} (75 MHz CDCl₃) δ 135.81, 132.22, 129.21, 126.24, 125.88, 124.77, 122.51, 122.26, 122.23, 122.03, 120.72, 120.58, 119.67, 119.65, 119.12, 24.18, 22.32, 8.61, 5.00; HRMS *m/z* for C₂₈H₃₆Sn, calcd 492.1839, found 492.1838.

Absorbance and Fluorescence Spectra and Quantum Yield Measurements. Absorbance spectra were recorded on a Perkin Elmer High Performance Lambda-6 spectrophotometer equipped with a double monochromator for reduced stray light. Fluorescence spectra were recorded on an SLM-8000C (SLM Aminco, Inc.) spectrofluorometer and corrected for the spectral response of the optical system. The

(54) Schulte-Frohlinde, D. *Chem. Unserer Zeit* **1990**, *24*, 37.

(55) Michalik, V. *Int. J. Radiat. Biol.* **1992**, *62*, 9.

(56) Cullis, P. M.; McClymont, J. D.; Malone, M. E.; Mather, A. N.; Podmore, I. D.; Sweeney, M. C.; Symons, M. C. R. *J. Chem. Soc., Perkin Trans. 2* **1992**, 695.

(57) Stille, J. K.; Wong, P. K. *J. Org. Chem.* **1975**, *40*, 532.

(58) Crouch, G. J.; Eaton, B. E. *Nucleosides Nucleotides* **1994**, *13*, 939.

correction factors were determined at GSU by technical support personnel from SLM Aminco, Inc. using a standard lamp whose energy output was traceable to NIST calibrations. The corrected emission spectra reported in this paper are plotted as relative detected-intensity versus wavelength. Solutions for fluorescence measurements typically contained 2–4 μM sample concentrations. The excitation wavelength for emission spectra and quantum yield measurements was 341 nm. Also for relative emission quantum yield measurements, the excitation bandwidth was 1 nm, and the absorbances of the two samples being compared were made nearly identical at an absorbance value of *ca.* 0.1. The fluorescence quantum yield (Φ_{em}) for pyrene butanoic acid (PBA; Molecular Probes, Inc., High Purity Grade, lot number 4721–1) in methanol (MeOH; EM Science, Omnisolv HR-GC grade) was measured to be 0.063 relative to 9,10-diphenylanthracene (Aldrich, 98%) in cyclohexane (Aldrich, Spectrochemical Grade) with $\Phi_{\text{em}} = 1.00$.⁵⁹ The emission quantum yields of pyrene-labeled uridine nucleosides were subsequently measured relative to PBA in MeOH. Appropriately oriented polarizers were used to eliminate the possible effects of nonisotropic fluorescence emission from the samples for both emission spectra and quantum yield measurements.⁶⁰ Also for samples with very weak emission, an indirect emission quantum yield method was used to increase the accuracy of the measurement.^{61–64} All samples used for emission spectra and quantum yield determinations were deaerated by bubbling with solvent-saturated argon for 20–30 min while being magnetically stirred. THF (Aldrich, HPLC Grade) was also used as noted for both emission quantum yield and lifetime measurements.

Fluorescence Lifetime Measurements. All fluorescence decays were recorded on a Tektronix SCD1000 transient digitizer (≤ 0.35 ns risetime calculated from the bandwidth, ≤ 120 ps risetime for a step input 0.5 times the vertical range) and wavelength was resolved with a 0.1-meter double monochromator (Instruments SA, Inc. model DH10) in additive dispersion. Slits (2-mm) were used producing an 8-nm bandpass. The 1200-grooves/mm holographic gratings were blazed at 450 nm. After passing through the monochromator, the emission was detected with a Hamamatsu 1564U microchannel plate (200 ps risetime). The excitation and emission beams were oriented at 90 degrees with respect to each other with the Glan-Thompson emission polarizer set at 54.7 degrees (“magic angle”) with respect to the vertical excitation-polarization to eliminate rotational diffusion artifacts in the emission lifetime measurements.⁶⁰ Emission for all lifetime measurements was excited at 355 nm with the third harmonic of an active-passive mode-locked Nd³⁺/YAG laser manufactured by Continuum, Inc. Typically 35– μJ excitation pulses of *ca.* 25-ps duration were collimated into a 3-mm diameter beam and passed through a second Glan-Thompson polarizer before entering the sample cuvette. Photon Technology Incorporated software was modified by the manufacturer to process 1000 data points per decay curve and was used to deconvolute the instrument response from the emission decay to yield exponential lifetime fits to the emission decay data. Emission lifetime tests were carried out on commercial samples of anthracene (Aldrich, 99+%) and 1-aminoanthracene (Aldrich, 99+%) which were dissolved in cyclohexane and degassed in o-ring sealed optical cells with three freeze–pump–thaw (FPT) cycles on a vacuum line (2×10^{-4} Torr). Recorded emission decays for these samples were fit with single exponential lifetimes of 5.1 and 22.5 ns, respectively, for anthracene and 1-aminoanthracene. These lifetimes agreed well with their respective literature values of 4.9 and 22.8 ns.⁵⁹ The generally observed temporal resolution of the emission kinetics system for multiexponential emission decays was *ca.* 0.2 ns; however, in ideal circumstances it was as good as *ca.* 50 ps after deconvolution (see below). All samples used for lifetime measurements were also degassed with three FPT cycles on a vacuum line as described above unless otherwise indicated.

(59) Beriman, I. B. *Handbook of Fluorescence Spectra of Aromatic Molecules*; Academic Press: New York, 1971.

(60) Lakowicz, J. R. *Principles of Fluorescence Spectroscopy*; Plenum Press: New York, 1986.

(61) Weber, G.; Teale, F. W. *Trans. Faraday Soc.* **1957**, *53*, 646.

(62) Parker, C. A.; Rees, W. T. *Analyst (London)* **1960**, *85*, 587.

(63) Parker, C. A. *Photoluminescence of Solutions. With Applications to Photochemistry and Analytical Chemistry*; Elsevier: Amsterdam and New York, 1968.

(64) Demas, J. N.; Crosby, G. A. *J. Phys. Chem.* **1971**, *75*, 991.

Table 1. Emission Lifetimes (ns) for **1** in MeOH and THF^a

MeOH Solvent (Emission Quantum Yield = 0.027)							
400 nm		430 nm		450 nm			
[0.90]	0.035 (23%)	[0.77]	0.042 (10%)	[0.66]	0.054 (8%)		
[0.09]	0.89 (59%)	[0.18]	0.98 (55%)	[0.29]	0.93 (64%)		
[0.01]	3.2 (18%)	[0.05]	2.2 (35%)	[0.05]	2.4 (28%)		
475 nm		520 nm		560 nm			
[0.69]	0.052 (10%)	[0.72]	0.039 (10%)	[0.46]	0.12 (10%)		
[0.28]	0.91 (70%)	[0.27]	0.90 (81%)	[0.53]	0.91 (90%)		
[0.03]	2.2 (20%)	[0.01]	1.9 (9%)				
THF Solvent (Emission Quantum Yield = 0.42)							
395 nm		430 nm		450 nm		495 nm	
[0.18]	0.3 (1%)	[0.24]	0.4 (2%)	[0.16]	0.8 (2%)	[0.12]	0.9 (2%)
[0.82]	6.7 (99%)	[0.76]	6.3 (98%)	[0.84]	6.2 (98%)	[0.88]	6.4 (98%)

^a [Fractional emission amplitude] emission lifetime (percent emission area). Lifetimes were measured in o-ring sealed cells which were degassed with three FPT cycles on a vacuum line.

χ values (technically the reduced χ -square statistic; the exact equation used is given as supporting information) for lifetime fits generally ranged from *ca.* 1–8; lower χ values were generally obtained at wavelengths near emission maxima. It is worth noting that considerable loss of emission intensity was suffered in these experiments so that wavelength resolved kinetics data could be obtained compared to the case if only long-pass emission filters had been used. Additionally, the interest in probing weak CT-emissions in the *ca.* 500-nm region as well as intense π, π^* emissions in the *ca.* 400-nm region necessarily meant that larger χ values were obtained in the red-region.

In general, the accuracy to which a lifetime component can be determined is proportional to the relative emission area of that component. For that reason relative area data are presented with the lifetime values. On the other hand, relative emission amplitudes are proportional to the number of emitting species with the corresponding lifetime; thus these data are also given. The combination of finite detector response time and small relative emission-areas (1–3%) for a number of the subnanosecond lifetime components presented in this work causes such values to be highly uncertain. Emission lifetime components ≥ 1 ns generally also have significant relative emission areas and are consequently much more reliable. However, whenever two emission lifetimes are less than a factor of 2 different for either bi- or triexponential decay processes, relative amplitude errors of $\pm 20\%$ and lifetime errors of ± 10 – 20% are common.⁶⁵ Typical errors for emission lifetimes that can be fit with only a single exponential are 2–4% for lifetimes ≤ 10 ns and 1–2% for lifetimes greater than 10 ns.

The emission kinetics data for **1** in MeOH (see Table 1) are unique in two ways. First, the longest emission decay component is only 2–3 ns long. This means that highly resolved risetime data and an accurate emission decay asymptote can be obtained on the same time scale (20 ns). Second, very large relative emission-amplitudes (*ca.* 0.5–0.9) and significant relative emission areas (*ca.* 10–30%) are present in this experiment for the ultrashort lifetime component. Under these circumstances the instrument response of the detection system after deconvolution appears to be *ca.* 50 ps (measured lifetimes for this component in Table 1 vary from 35–54 ps at seven wavelengths in the 390–560 nm range, data for only six wavelengths are shown).

Emission kinetics were analyzed with the following criteria in mind: (1) reproducibility of a given measurement, (2) continuity of the variation of lifetimes as emission wavelength was varied (a global analysis), and (3) consistency of lifetime components found by fitting data from several time ranges. In addition to these criteria, Ockham's razor was used to demand that a significant improvement in χ be made before an additional lifetime component be added. Generally, this was at least a 0.5–1.0 lowering of χ . We did, however, find many times that the number of required lifetimes was robust. That is, an attempt to add another lifetime just repeated a previous lifetime

(65) Vix, A.; Lami, H. *Biophys. J.* **1995**, *68*, 1145.

component or an attempt to remove a lifetime component gave a very much larger χ .

The general fitting procedure began by insuring that each emission lifetime was recorded on a sufficiently coarse time scale so that its emission decayed into the noise (typically ± 4 – 8 counts compared to 10 000–12 000 counts in the signal's peak after background subtraction). These decay data were fit first, and their longest lifetime component was then used as a fixed lifetime in fits of data taken on finer time scales. The finer time scales allowed better resolution of the faster decay components. The finest time scale used in this work was 20 ns, corresponding to one time point every 20 ps. Each kinetics trace on each time scale recorded 1000 data points; all fits used all 1000 points; and all data curves that were fit were themselves the result of averaging 1000 photoexcitation events as well as 1000 background events and subtracting the latter from the former. Plots of nine of the emission decays acquired for this study along with fits to them and their corresponding χ values are available as supporting information.

Results and Discussion

UV-vis Spectra and Emission Lifetimes for 1. Figure 1 compares the emission and absorbance spectra for pyrene butanoic acid (PBA) in MeOH (top) and **1** in MeOH (middle) and in THF (bottom). Conjugation of the pyrenyl chromophore in **1** with the π -system of dU causes only a small red-shift in the absorbance maximum of the second excited singlet, π, π^* state of pyrene in MeOH from 341 nm for PBA to 342 nm for **1**. However, there is extensive broadening of the vibrational fine-structure of this electronic transition for **1** compared to the well-resolved vibrational bands for PBA. Additionally, this broadening for **1** is accompanied by loss of molar extinction at this same π, π^* transition from $43\,100\text{ M}^{-1}\text{ cm}^{-1}$ for PBA⁶⁶ to $25\,800\text{ M}^{-1}\text{ cm}^{-1}$ for **1**. The π, π^* emission for PBA in MeOH originates from the first excited singlet state and shows vibrational fine-structure as is common for many PAH compounds.^{4,8,67} The structureless emission for **1** in MeOH, however, is red-shifted and much broader than for PBA. Additionally, the emission maximum for **1** in MeOH is approximately in the center of its emission spectrum, while that of PBA is located at its high energy edge. Clearly the broad emission of **1** in MeOH is not characteristic of PAH π, π^* emission. Rather, it is very much like that seen in pyrene exciplexes, pyrene heteroexciplexes, and inorganic complexes with lowest energy metal-to-ligand (MLCT) excited states such as $\text{Ru}(2,2'\text{-bipyridine})_3^{2+}$.^{15,68–78}

To the extent the emitting state of **1** in MeOH has more polar character than nearby π, π^* states, changing the solvent's dielectric constant (η) from 33.6 (MeOH) to 7.6 (THF) is

- (66) Landon, T. (private communication, Molecular Probes, Inc.).
 (67) Perichon, J. In *Encyclopedia of Electrochemistry of the Elements, Organic Section*; Bard, A. J., Lund, H., Eds.; Marcel Dekker, Inc.: New York and Basel, 1978; Vol. 11, p 108.
 (68) Vitukhnovsky, A. G.; Sluch, M. I.; Warren, J. G.; Petty, M. C. *Chem. Phys. Lett.* **1991**, *184*, 235.
 (69) Inai, Y.; Sisido, M.; Imanishi, Y. *J. Phys. Chem.* **1990**, *94*, 8365.
 (70) Koshioka, M.; Misawa, H.; Sasaki, K.; Kitamura, N.; Masuhara, H. *J. Phys. Chem.* **1992**, *96*, 2909.
 (71) Lumpkin, R. S.; Kober, E. M.; Worl, L. A.; Murtaza, Z.; Meyer, T. J. *J. Phys. Chem.* **1990**, *94*, 239.
 (72) Rillema, D. P.; Blanton, C. B.; Shaver, R. J.; Jackman, D. C.; Boldaji, M.; Bundy, S.; Worl, L. A.; Meyer, T. J. *Inorg. Chem.* **1992**, *31*, 1600.
 (73) Lianos, P.; Zana, R. *J. Phys. Chem.* **1980**, *84*, 3339.
 (74) Bohorquez, M. D.; Patterson, L. K. *Langmuir* **1993**, *9*, 2097.
 (75) Letsinger, R. L.; Wu, T. *J. Am. Chem. Soc.* **1994**, *116*, 811.
 (76) Nemeth, S.; Jao, T.-C.; Fendler, J. H. *J. Photochem. Photobiol. A* **1994**, *78*, 229.
 (77) Creutz, C.; Chou, M.; Netzel, T. L.; Okumura, M.; Sutin, N. *J. Am. Chem. Soc.* **1980**, *102*, 1309.
 (78) van Houte, L. P. A.; van Grondelle, R.; Retel, J.; Westra, J. G.; Zinger, D.; Sutherland, J. C.; Kim, S. K.; Geacintov, N. E. *Photochem. Photobiol.* **1989**, *49*, 387.

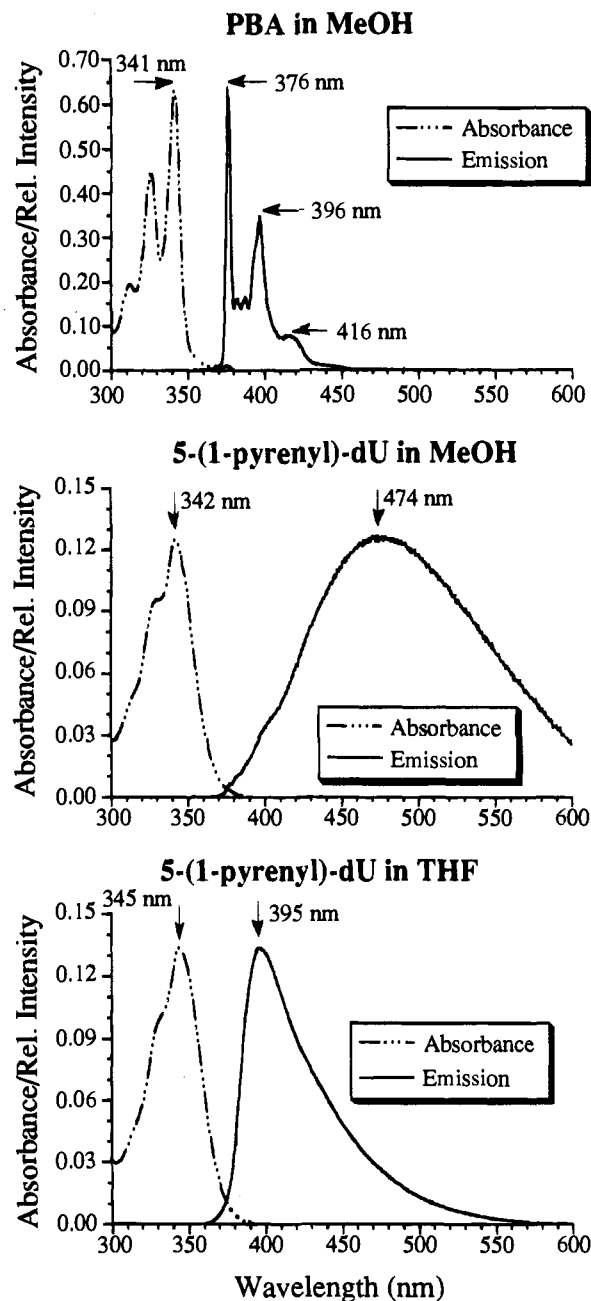


Figure 1. Spectral plots of both absorbance versus wavelength and normalized, corrected emission intensity versus wavelength for (top) PBA in MeOH, (middle) 5-(1-pyrenyl)-dU, **1**, in MeOH, and (bottom) **1** in THF. The concentrations of PBA in MeOH for absorbance and emission, respectively, were 1.5×10^{-5} and 2.4×10^{-6} M; the concentration of **1** in MeOH for both absorbance and emission was 4.9×10^{-6} M; the concentration of **1** in THF for both absorbance and emission was 4.7×10^{-6} M. [For **1** in MeOH $\epsilon(342\text{ nm}) = 25\,800\text{ M}^{-1}\text{ cm}^{-1}$, and in THF $\epsilon(345\text{ nm}) = 26\,800\text{ M}^{-1}\text{ cm}^{-1}$.]

expected to raise its energy relatively more than it raises the energy of nearby π, π^* states. Indeed the middle and bottom panels of Figure 1 show that while the π, π^* absorbance maximum red-shifts only slightly from 342 to 345 nm on going from MeOH to THF, the emission maximum blue-shifts 80 nm, from 474 to 395 nm. Significantly, the spectral shape of the emission of **1** in THF suggests that it is vibrationally broadened π, π^* emission reminiscent of that seen for PBA in MeOH.

The emission quantum yield measured here for PBA in MeOH is 0.063, while those for **1** in MeOH and THF, respectively, are 0.027 and 0.42. There are also significant lifetime differences in MeOH between the π, π^* emission of

PBA and the broad emission of **1**. PBA's emission in MeOH is biexponential with lifetime components of 125 [0.45 relative emission amplitude] and 231 ns [0.55 relative emission amplitude]. The reason PBA emission in MeOH exhibits two lifetimes is not clear; however, it is not necessary to know this reason for this study. It is true, though, that when PBA is dissolved in aqueous phosphate buffer at pH 9.0 the lifetime pattern changes to the following, 95 ns [0.90 relative emission amplitude] and 193 ns [0.10 relative emission amplitude]. PBA's UV-vis spectral and emission lifetime properties are presented here only to show the kind of behavior a 1-alkyl-pyrenyl ligand's π,π^* excited state might reasonably exhibit in the absence of ET quenching. In contrast to the long emission lifetimes of PBA, the kinetics data in Table 1 show that the emission decay of **1** in MeOH is triexponential with its longest lifetime component only ca. 2–3 ns. Based on considerations of the emission band-shape of **1** and the energy of a pyrene $^{+}$ /dU $^{-}$ CT state (see below), it is reasonable to assign the broad 470-nm emission from **1** as originating from a pyrene-to-uridine CT state. This assignment is also consistent with an earlier report of CT-emission (or heteroexciplex emission) in another PAH/nucleoside adduct formed from the covalent binding of the carcinogen 2-aminofluorene (AF) to the C8 position of dG to make dG-C8-AF.⁷⁸ At room temperature, this adduct's fluorescence was also broad and structureless with a maximum at 460 nm in aqueous mixtures, shifting to 415 nm in solvents of lower polarity. In water a single short lifetime of 0.08 ns was seen. At 77 K this adduct's emission was structured and characteristic of π,π^* emission in AF. Note, however, the ET product in dG-C8-AF is dG $^{+}$ /AF $^{-}$,^{20,25,79} while in pyrenyl-dU it is pyrene $^{+}$ /dU $^{-}$.

For the emission lifetime measurements reported in Table 1, samples of **1** were dissolved at a 9.9×10^{-6} M concentration in MeOH and at 5.0×10^{-6} M in THF. Several points can be made concerning this lifetime data. One, the longest emission component (2–3 ns) progressively loses both relative emission area and relative emission amplitude as the wavelength increases until it vanishes at 560 nm. This is exactly the spectral behavior which one would expect for a π,π^* state. In contrast, the 0.9-ns component exhibits a progressive growth in both relative emission area and amplitude as wavelength increases. This spectral response matches that of the emission spectrum shown for **1** in MeOH in the middle panel of Figure 1 and identifies the 0.9-ns component as arising from CT-emission. The ultrashort component (≤ 50 ps) has contributions from both the π,π^* and CT states. This can be seen first by noting that one would not expect π,π^* emission at 560 nm, yet 50% of the emission amplitude at this wavelength has an apparent decay lifetime of 120 ps. Second 90% of the relative emission amplitude at 400 nm corresponds to the ≤ 50 -ps component, while the relative percentage of the amplitude for this same component progressively drops to 46% at 560 nm. This establishes that the ET quenching process has at least two characteristic lifetimes, ≤ 50 ps and 2–3 ns. Also, the charge recombination step in MeOH itself has two characteristic lifetimes, ≤ 50 ps and 0.9 ns.

The conclusion that the pyrene-labeled nucleoside **1** has a number of different conformers in MeOH and that some of these exhibit π,π^* ET-quenching rates that vary by at least 60-fold seems unavoidable. Similarly, at least a 20-fold variation in charge-recombination times appears to be present. Mechanical molecular models show that very different relative orientations of the deoxyribose, uracil, and pyrene groups are possible.

Additionally, it seems plausible that the time to reconfigure these large groups from one type of relative orientation to another by means of random librations could take as long as several nanoseconds. Whether any particular intramolecular interactions (e.g., hydrogen bonds) also stabilize certain conformations is not clear but cannot be ruled out.

The emission decay kinetics of **1** in THF are simpler than in MeOH in two ways. First, biexponential kinetics are adequate to fit them rather than triexponential ones. Second the pattern of relative emission amplitudes is roughly the same from 395 to 495 nm: 10–20% of the emission amplitude decays in ≤ 1 ns and ca. 80–85% of it decays in ca. 6.5 ns. The variation with wavelength of the lifetimes measured for the longest emission component for **1** in THF illustrates the measurement error in this time region and is consistent with the errors found in comparisons of lifetime measurements for known compounds with their literature values (see above).

Lowering the solvent's dielectric constant by changing from MeOH to THF affects the emission of **1** in three ways. One, its quantum yield increases 16-fold. Two, its spectrum changes character from CT to π,π^* . Three, its pattern of amplitude variation with wavelength for different lifetime components changes from two-state to one-state behavior. However, in THF the emission decay of **1** at all wavelengths still retains evidence of subnanosecond relaxations (10–20% relative emission amplitude). Presumably these ultrafast relaxations show that a certain amount of CT quenching is still occurring in THF. How much longer lived the 6.5-ns component itself would be in complete absence of CT quenching is not known; however, an upper limit for this lifetime is ca. 15 ns.

Free Energies for Excited-State Electron Transfer Quenching. Electrochemical data on the oxidation of pyrene and reduction of dT (and by extension dU) can be combined with the energy of the first excited π,π^* state of **1**, $E_{o,o}(\text{pyrene}^*)$, to estimate the free energy for electron transfer quenching of pyrene * , $\Delta G^\circ(\text{ET})$, according to eq 1⁸⁰

$$\Delta G^\circ(\text{ET}) = E^\circ(\text{pyrene}^*/\text{pyrene}) - E^\circ(\text{dU}/\text{dU}^-) - E_{o,o}(\text{pyrene}^*) + w(r)$$

where E° is a reduction potential and $w(r)$ is a coulombic interaction term between oxidized pyrene and reduced dU which represents free energy due to separating the ionic products at a distance r relative to each other, $w(\infty) = 0$.^{81,82} Generally in very polar media the coulombic term is less than ca. 0.1 eV and will be neglected here.^{25,48,81,83,84}

Although the redox potentials of pyrene and dU in **1** will not be exactly the same as those of pyrene and dU in isolation, the redox values of the isolated subunits can provide a useful estimate of the free energy for this ET reaction. The reduction potentials (versus a saturated calomel electrode, SCE) in polar solvents for the pyrene $^{+}$ /pyrene and dU/dU $^{-}$ couples, respectively, are +1.28 and -1.45 V.^{20,24,67,85,86} When these values are combined with the ca. 3.25 eV of excited state energy of **1** according to eq 1, $\Delta G^\circ(\text{ET})$ is estimated to be -0.52 eV. Thus

(80) Rehm, D.; Weller, A. *Isr. J. Chem.* **1970**, *8*, 259.

(81) Sutin, N.; Brunschwig, B. S.; Creutz, C.; Winkler, J. R. *Pure Appl. Chem.* **1988**, *60*, 1817.

(82) Brunschwig, B. S.; Ehrenson, S.; Sutin, N. *J. Phys. Chem.* **1986**, *90*, 3657.

(83) Sutin, N. In *Electron Transfer in Inorganic, Organic, and Biological Systems*; Bolton, J. R., Mataga, N., McLendon, G., Eds.; American Chemical Society: Washington, D.C., 1991; p 25.

(84) Marcus, R. A.; Sutin, N. *Biochim. Biophys. Acta* **1985**, *811*, 265.

(85) Faraggi, M.; Klapper, M. H. *J. Chim. Phys.* **1994**, *91*, 1054.

(86) Steenken, S.; Telo, J. P.; Novais, H. M.; Candeis, L. P. *J. Am. Chem. Soc.* **1992**, *114*, 4701.

(79) Shafirovich, V. Y.; Courtney, S. H.; Ya, N.; Geacintov, N. E. *J. Am. Chem. Soc.* **1995**, *117*, 4920.

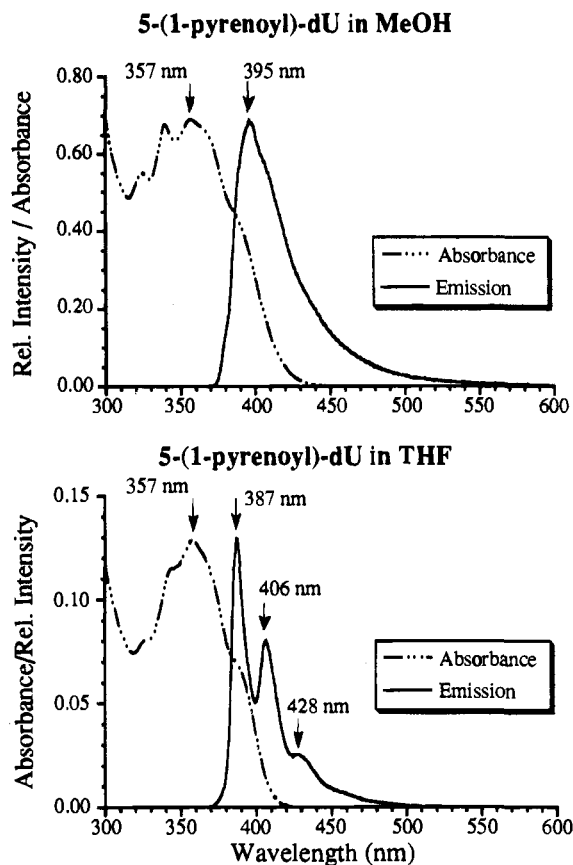


Figure 2. Spectral plots of both absorbance versus wavelength and normalized, corrected emission intensity versus wavelength for 5-(1-pyrenoyl)-dU, **2**, in (top) MeOH and (bottom) THF. For **2** in MeOH, concentration = 1.0×10^{-4} M for absorbance and 1.6×10^{-5} M for emission; in THF, concentration = 1.5×10^{-5} M for both absorbance and emission. [In MeOH $\epsilon(357 \text{ nm}) = 6680 \text{ M}^{-1} \text{ cm}^{-1}$, and in THF $\epsilon(357 \text{ nm}) = 8570 \text{ M}^{-1} \text{ cm}^{-1}$.]

there is a large driving force in polar solvents for ET quenching of pyrene* in **1**, which is consistent with the striking absence of π, π^* emission features in the 370–500 nm range in Figure 1 for **1** in MeOH. (In fact a slight “bump” at 395 nm on the rising slope of this CT emission band (middle panel of Figure 1) is barely visible. This “emission bump” is likely due to the small amount (1–5% relative emission amplitude) of 2–3 ns lived π, π^* emission noted in Table 1 for **1** in MeOH.)

UV-vis Spectra and Emission Lifetimes for 2. Figure 2 presents absorbance and emission spectra for 5-(1-pyrenoyl)-dU, **2**, in MeOH and THF. For **2** in MeOH, both the absorbance and emission spectra are similar to those of 1-pyrenecarboxaldehyde in polar solvents. Conjugation of the carbonyl group with the π -system of pyrene has several important consequences.^{7,87} One, n, π^* states are now near the two lowest energy π, π^* states. Two, the two lowest energy π, π^* states are both lowered in energy, but the higher energy state is lowered more than the lowest energy one so spectral crowding occurs. This crowding and lowering of π, π^* levels is seen in the absorbance spectra of **2** in MeOH in that the first strong absorbance band (a shoulder) begins *ca.* 390 nm, whereas the S_2 absorbance of **1** in MeOH has its maximum at 342 nm. On changing solvent from MeOH to THF for **2**, small changes occur in the vibrational band absorbances to the blue of 357 nm, and the onset of absorbance blue-shifts by *ca.* 10 nm, from 420 nm in MeOH to 410 nm in THF. In both solvents the emission

Table 2. Emission Kinetics (ns) for **2** in MeOH and in THF^a

MeOH Solvent (Emission Quantum Yield = 0.002)		
382 nm	393 nm	400 nm
[0.20] 0.5 (1%)	[0.30] 0.3 (2%)	[0.57] 0.7 (10%)
[0.80] 9.0 (99%)	[0.70] 8.7 (98%)	[0.43] 8.7 (90%)
430 nm	450 nm	495 nm
[0.36] 0.6 (4%)	[0.34] 0.5 (3%)	[0.68] 0.4 (15%)
[0.64] 8.5 (96%)	[0.66] 8.3 (97%)	[0.11] 1.8 (10%)
		[0.21] 7.2 (75%)
THF Solvent (Emission Quantum Yield = 0.028)		
387 nm	406 nm ^b	428 nm ^b
[0.32] 0.4 (2%)	[0.32] 0.7 (3%)	[0.12] 1.6 (2%)
[0.58] 9.2 (61%)	[0.55] 8.8 (56%)	[0.73] 6.8 (50%)
[0.08] 21 (21%)	[0.11] 15 (19%)	[0.13] 16 (20%)
[0.02] 92 (16%)	[0.02] 96 (22%)	[0.02] 96 (28%)
	450 nm ^b	
	[0.30] 1.1 (5%)	
	[0.63] 6.4 (66%)	
	[0.06] 15 (15%)	
	[0.01] 92 (14%)	

^a [Fractional emission amplitude] emission lifetime (percent emission area). Experimental conditions as noted in Table 2. ^b Shorter (<0.5 ns) components are also present. While fits to the emission decay data with five lifetimes give slightly lower χ values, the pattern of lifetimes for decays > 5 ns is not significantly changed.

has π, π^* character; however, only in THF is the vibrational structure well resolved.

Table 2 reports the emission lifetimes observed for **2** in MeOH and THF at a number of wavelengths. The emission quantum yields for **2** in MeOH and THF, respectively, are 0.002 and 0.028. These can be compared with the quantum yield of 1-pyrenecarboxaldehyde in MeOH, 0.07–0.15.^{88–90} Emission lifetimes have also been reported for 1-pyrenecarboxaldehyde in MeOH as 1.95⁹⁰ and 1.6 ± 0.1 ns.⁸⁹ For the emission lifetime measurements reported in Table 2, samples of **2** were dissolved in MeOH and THF, respectively, at 3.1×10^{-5} and 2.5×10^{-5} M concentration.

The emission quantum yield increase for **2** on going from MeOH to THF solvent is consistent with less ET quenching of π, π^* emission on going from a higher to a lower dielectric solvent (see below) and is inconsistent with an emission yield variation due to changing the location of the lowest energy n, π^* state. When n, π^* states are very near or below π, π^* states in substituted aromatic systems, π, π^* emission is quenched.^{87,91} For **2** the n, π^* state is expected to be higher in MeOH (due to solvent proton donation) than in THF, and yet the emission quantum yield is lower in MeOH than in THF.

Ongoing picosecond transient absorbance kinetics studies of **2** in MeOH in our laboratory demonstrate the formation of pyrene⁺⁺ following photoexcitation as judged by the appearance of the very strong, pyrene cation absorbance at 460 nm in ≤ 30 ps followed by its decay in 20–70 ps (the decay lifetime without deconvolution is 67 ± 3 ps).⁹² Control experiments show that the laser excitation power in this experiment is insufficient to photoionize PBA directly. Thus the very low emission quantum yield of **2** in MeOH is due to the fact that most conformers of **2** undergo ET quenching of their π, π^* states in ≤ 30 ps.

The emission lifetimes for **2** in MeOH in Table 2 show

(88) Oton, J. M.; Acuna, A. U. *Photochem. Photobiol.* **1980**, *31*, 342.

(89) Dederen, J. C.; Coosemans, L.; De Schryver, F. C.; Van Dormael, A. *Photochem. Photobiol.* **1979**, *30*, 443.

(90) Kalyanasundaram, K.; Thomas, J. K. *J. Phys. Chem.* **1977**, *81*, 2176.

(91) Baliah, V.; Pillay, M. K. *Indian J. Chem.* **1971**, *9*, 815.

(92) Netzel, T. L.; Nafisi, K.; Headrick, J.; Eaton, B. E. *J. Phys. Chem.* Submitted for publication.

(87) Lianos, P.; Lux, B.; Gerard, D. *J. Chim. Phys. Phys. Chim. Biol.* **1980**, *77*, 907.

predominantly biexponential decays. In fact only in the red-region at 495 nm is there an indication of triexponential kinetics. (Two lifetimes do not fit the emission decay kinetics here. At 430 and 450 nm, in contrast, slightly better kinetics fits are obtained with three lifetimes than with two, but the reductions in χ are not large.) Significantly, 495 nm is exactly where CT emission would most likely dominate π, π^* emission, and twice the relative amplitude of subnanosecond emission decay is present here compared to that seen at nearly all of the other wavelengths in Table 2. The finite response time of the emission detector cannot accurately record the ≤ 30 ps π, π^* quenching step for the large majority of conformers of **2** in MeOH. Thus the relative emission amplitude of the subnanosecond decay process is severely underestimated with respect to the 8.5-ns emission decay process.

In contrast to **1** in MeOH, **2** in the same solvent gives no spectral indication of emission from the CT product, pyrene⁺⁺/dU⁻, in spite of its low emission quantum yield. The simplest explanation is that the CT-product and ground electronic states are more distorted (shifted) with respect to each other for **2** than they are for **1**. It is likely that the breadth of the π, π^* emission spectra for **1** in THF and for **2** in MeOH and THF reflect the couplings of the dipolar emitting states with the phonon modes of the solvent. If this model is correct, the fact that the emission spectrum of **1** in THF is much broader than that of **2** in THF and shows no vibrational fine structure implies that the emitting state of **1** in this solvent has more charge-separation character. That the emission spectrum of **2** broadens on going from THF to MeOH is consistent with this model, since MeOH is both a more polar and a hydrogen donating solvent and thus can interact more strongly with a polar excited state than can THF. Comparison of the π, π^* emission spectrum of **2** in MeOH with that of PBA in MeOH in terms of this model implies that the emitting state of **2** has more polar character than does the pure π, π^* state of PBA. Detailed quantum mechanical calculations on compounds **1** and **2** would be of interest in this regard. A quantum model of spectral broadening due to π, π^* - and CT-state mixing, which also supports the above conclusions concerning the degree of polar character of the emitting states of **1** and **2**, was recently presented for a series of tetrakis(*N*-methylpyridyl) porphyrins.⁹³ However, in this latter model solvent interaction with the emitting state was neglected.

Figure 2 shows that the emission spectrum of **2** has well resolved vibrational structure in THF. The emission spectra of **3**, the 3',5'-bis(silyl)-substituted analog of **2**, have also been recorded in MeOH, THF, and cyclohexane. In each of these solvents, **3** has the same well resolved vibrational bands at 387, 406, and 428 nm with very similar relative intensities as does **2** in THF. The striking difference between the emissions for these two compounds in THF is that their quantum yields are 2.8×10^{-2} and 5.4×10^{-5} , respectively, for **2** and **3**. The much lower emission quantum yield of **3** compared to **2** in THF likely reflects an additional radiationless decay channel in **3** due to the silicon substituents. This decay channel could be increased intersystem crossing between the singlet and triplet π, π^* manifolds of the pyrenyl-ligand.

Both **2** and **3** show increased emission quantum yields upon decreasing the solvent's dielectric constant. For **2** changing from MeOH ($\eta = 33.6$) to THF ($\eta = 7.6$) increases the quantum yield from 2×10^{-3} to 2.8×10^{-2} , 14-fold; for **3** changing from THF to cyclohexane ($\eta = 2.0$) increases the quantum yield from 5.4×10^{-5} to 1.3×10^{-3} , 24-fold. The quantum yield of **3** in MeOH has not been measured, but its weak emission signal in this solvent indicates that its emission yield is similar to that in THF. The solvent dependence of the emission quantum

Table 3. Emission Kinetics for **3** in MeOH^a

387 nm		400 nm		406 nm	
[0.37]	2.1 (10%)	[0.46]	0.12 (2%)	[0.35]	2.9 (16%)
[0.63]	10.7 (90%)	[0.24]	1.8 (12%)	[0.63]	9.1 (84%)
		[0.30]	9.6 (86%)		
450 nm			495 nm		
[0.92]	0.2 (38%)		[0.90]	<0.1 (47%)	
[0.06]	1.6 (18%)		[0.09]	0.45 (27%)	
[0.02]	8.1 (44%)		[0.01]	4.2 (26%)	

^a [Fractional emission amplitude] emission lifetime (percent emission area). Experimental conditions as noted in Table 2. Emission quantum yields for **3** in THF and cyclohexane are, respectively, 5.4×10^{-5} and 1.3×10^{-3} .

yields for **2** and **3** is consistent with the expected solvent-dielectric dependence of ET quenching rates for normal ET reactions, i.e., slower rates in lower dielectric solvents due to increased (less negative) free energy of ET between the π, π^* and CT-product states.^{81,83,84}

It is perhaps useful to mention here that solvents have other important properties besides their dielectric response. For example, MeOH is both a powerful proton donor and a high dielectric solvent, while THF and cyclohexane are low dielectric media and poor proton donors. Thus changing from MeOH to THF as a solvent changes two important solvent properties. In MeOH both protonation of dU⁻ as well as dielectric stabilization of the pyrene⁺⁺/dU⁻ CT-product can contribute to lowering the energy of the CT state relative to the lowest energy π, π^* states of **1**, **2**, and **3**. The important consequence of both of these effects for this work is that in MeOH a pyrene-to-uridine CT state is expected to have a lower energy than in THF. Ongoing studies are attempting to determine the relative importance of proton donation and dielectric stabilization to lowering the energy of the pyrene⁺⁺/dU⁻ CT-state.

Table 2 shows that (consistent with the above conclusion that ET quenching of π, π^* emission is occurring for **2** and **3** in THF) the emission kinetics for **2** in THF are at least quadruply exponential. Additionally, the longest emission lifetimes last ca. 95 ns. However, only about 10% of the emission amplitude decays with lifetimes greater than 10 ns. Approximately 90% of the emission amplitude decays on the same time scale as it did for **2** in MeOH. Most likely a complex interplay of electronic coupling and solvent-dependent reorganization energy differences for different conformers of **2** is responsible for the unusually complex emission kinetics of **2** in THF. Electrochemical measurements on **2** and **1** in the same solvents would be useful for learning more about the ET quenching reactivity differences between them. For example, the emission quantum yields of **2** in both MeOH and THF are ca. 15-fold lower than those of **1** in these same solvents. This suggests that $\Delta G^\circ(\text{ET})$ for **2** is more negative than for **1**.

Emission Lifetimes for Bis(silyl) 2. Emission kinetics for 3',5'-bis(*tert*-butyldimethylsilyl)-5-(1-pyrenoyl)-dU, **3**, in MeOH at a number of wavelengths are presented in Table 3. In this sample the 3',5'-H atoms of **2** are replaced with much larger *tert*-butyldimethylsilyl groups.

For the emission lifetime measurements reported in Table 3, the samples of **3** were dissolved in MeOH at 8.4×10^{-5} M concentration. For this sample triexponential emission decay kinetics are present at most of the wavelengths in Table 3. The exceptions are at 387 and 406 nm which correspond to π, π^* vibrational peaks. This wavelength dependent kinetics pattern suggests that **3** is conformationally heterogeneous on the ≤ 10 ns time scale in MeOH. This conclusion is also supported by examination of the absorbance and emission origins for **3** in

MeOH, THF, and cyclohexane (spectra not shown). In all three solvents, a well resolved first vibrational peak is found in emission at 387 nm. In contrast as the solvent is changed in this series, the onset of absorbance blue-shifts: 440 nm (MeOH), 416 nm (THF), and 412 nm (cyclohexane). The growth in the sharpness and prominence of the first absorbance band in this series of solvents is even more dramatic: slowly rising with an unresolved shoulder in MeOH, moderately rising with a clear shoulder in THF, and sharply rising with a well-resolved peak at 393 nm in cyclohexane. A similar blue-shift of absorbance is shown in Figure 2 for **2** on changing solvent from MeOH to THF. A blue-shift of π,π^* absorbances is expected as solvent dielectric is decreased.^{7,91,94} The fact that the positions of the emission origin and its next two vibrational bands are invariant with respect to change of solvent suggests that these high energy emission features arise from a subset of conformers with poor π,π^* emission quenching and not from the bulk of the sample. (The emission spectra in different solvents do vary with respect to each other in the red-wavelength region beyond 430 nm.)

That the emission spectra of **2** and **3** reflect more heavily the microenvironments of the longest-lived conformers and that the absorbance spectra reflect more nearly the average conformer's environment are not surprising. With this idea in mind, however, one can notice two unusual features of the absorbance and emission spectra of **2** in Figure 2. First, although the onset of absorbance blue-shifts from 425 to 410 nm on going from MeOH to THF, the onset of emission is unchanged (or even red-shifts slightly). Second, the location of the emission peak at 387 nm for **2** in THF is over 10 nm blue of the place one would expect it to be given the onset of absorbance well before 400 nm. Similarly, for **3** in MeOH the first emission peak is over 25 nm blue of the onset of absorbance, and for **3** in cyclohexane the first emission peak at 387 nm is actually blue of the first absorbance peak at 393 nm. The extremely low emission quantum yields for **3** mean that only a very small fraction ($\leq 0.1\%$) of excited molecules emit. This sets the stage for a striking disparity between absorbance and emission origins. In contrast, molecules with high emission yields are more likely to show reasonable Stokes shifts.

The weight of the spectral and emission kinetics data for **1**, **2**, and **3** strongly supports the conclusion that each of these nucleosides has multiple conformers in solution on the 10–100 ns timescale depending upon solvent. In addition, the π,π^* ET-quenching times for a single pyrene-labeled nucleoside vary from ≤ 30 ps (for **2** in MeOH) to ≥ 95 ns (for **2** in THF where subnanosecond ET quenching times are also present), more than 3000-fold. For **1** in MeOH, ET quenching times vary from ≤ 50 ps to 3 ns, *ca.* 60-fold. Whether only a few conformers are present (or dominate) for each nucleoside or whether polymodal distributions of conformers are present is not known. The longest and shortest emission lifetimes for **3** in MeOH in Table 3 are not very different from those for **2** in MeOH in Table 2. The presence of a 2-ns lifetime emission decay with 25–30% relative amplitude for **3** in MeOH is a new kinetics feature for **3** which is not prominent for **2** in MeOH. After the fact it appears that this kinetics difference is due to the 3',5'-bis(silyl) substitution in **3** versus the 3',5'-H substitution in **2**. However, how the distributions of conformers differ for these two nucleosides is not known.

Conclusions

Both the absence of π,π^* emission and the presence of CT (or heteroexciplex) emission are striking and surprising for **1** in MeOH. Thermodynamic analysis suggests that the CT photoproduct is most likely pyrene⁺/dU⁻. Although inter-

molecular pyrene excimer emission is spectrally similar to the CT emission of **1**, it is impossible for two pyrene-labeled nucleosides to diffuse together in 50 ps in a solution with a nucleoside concentration of 2.4×10^{-6} M.⁹ At this nucleoside concentration, a bimolecular process such as pyrene excimer formation would require at least 20 μ s (assuming a bimolecular quenching constant $\leq 2 \times 10^{10}$ M⁻¹ s⁻¹).^{9,95} The CT emission kinetics of **1** in MeOH are complex, but their spectral variation suggest that the CT state has both ≤ 50 -ps and 0.9-ns relaxation lifetimes. It is the 0.9-ns lived CT states, therefore, which are largely responsible for the steady-state emission of **1** in MeOH. While the π,π^* states also exhibit biexponential quenching kinetics with lifetimes of ≤ 50 ps and 2–3 ns, the emission from the few long-lived π,π^* states is dominated at all wavelengths by the CT emission.

Lowering the solvent's dielectric constant by changing from MeOH to THF affects the emission of **1** in three ways. One, its quantum yield increases 16-fold from 0.027 to 0.42. Two, its spectrum changes character from CT to π,π^* . Three, its pattern of amplitude variation with wavelength for different lifetime components changes from two-state to one-state behavior. However, in THF the emission decay of **1** at all wavelengths still retains evidence of subnanosecond relaxations (10–20% relative emission amplitude). Presumably these ultrafast relaxations show that a certain amount of ET quenching is still occurring in THF.

For all three pyrene-labeled nucleosides studied here, increasing the solvent's dielectric constant decreases the emission quantum yield. For **1** changing from THF ($\eta = 7.6$) to MeOH ($\eta = 33.6$) decreases the quantum yield from 0.42 to 0.027, 16-fold; for **2** changing from THF to MeOH decreases the quantum yield from 2.8×10^{-2} to 2×10^{-3} , 14-fold; for **3** changing from cyclohexane ($\eta = 2.0$) to THF decreases the quantum yield from 1.3×10^{-3} to 5.4×10^{-5} , 24-fold. The solvent dependence of the emission quantum yields for all three is consistent with the expected solvent-dielectric dependence of ET quenching rates for normal ET reactions, i.e., faster ET rates in higher dielectric solvents due to decreased (more negative) free energy of ET between the π,π^* and CT-product states.^{81,83,84}

The spectral and emission kinetics data for all three nucleosides strongly support the conclusion that each has multiple conformers in solution in 10–100 ns time range depending upon solvent. Additionally, the ET quenching times for a single pyrene-labeled nucleoside vary from ≤ 30 ps (for **2** in MeOH) to ≥ 95 ns (for **2** in THF where subnanosecond quenching times are also present), more than 3000-fold. For **1** in MeOH, ET quenching times vary from ≤ 50 ps to 3 ns, *ca.* 60-fold, and charge recombination times vary from ≤ 50 ps to 0.9 ns, *ca.* 20-fold. These results suggest that the relative orientation of the pyrene and uridine π -systems plays a crucial role in determining the rates of both ET quenching of pyrene* and charge-recombination in the photoproduct. Whether only a few conformers are present (or dominate) for each nucleoside or whether polymodal distributions of conformers are present is not known.

Although the lifetimes the pyrene⁺/dU⁻ CT products of **1** and **2** are short (as long as 0.9 ns for **1** and 20–70 ps for **2** both in MeOH), it is not clear whether or not these nucleosides will exhibit only charge recombination after photoexcitation

(93) Vergeldt, F. J.; Koehorst, R. B. M.; Hoek, A. v.; Schaafsma, T. J. *Phys. Chem.* **1995**, *99*, 4397.

(94) Lianos, P.; Mukhopadhyay, A. K.; Georghiou, S. *Photochem. Photobiol.* **1980**, *32*, 415.

(95) Duhamel, J.; Winnik, M. A.; Baros, F.; Andre, J. C.; Martinho, J. M. G. *J. Phys. Chem.* **1992**, *96*, 9805.

when substituted into DNA oligomers and duplexes. For example, if a guanine base were adjacent to **2** in an oligonucleotide, a dG^{*+}/dU^{*-} CT product would be thermodynamically favored over $pyrene^{*+}/dU^{*-}$. Whether or not secondary charge shift processes such as from $pyrene^{*+}$ to dG or from dU^{*-} to dC can compete with charge recombinations within pyrene-labeled uridine nucleosides in DNA oligomers and duplexes are important questions.^{43-45,51,96-98} How the competitions among the charge recombination and charge shift processes are affected by change of solvent (e.g., from polar protic to polar nonprotic for single strands of DNA) and change of DNA structure (e.g., from single strand, random coil to duplex in water) are also of interest.

(96) Brun, A. M.; Harriman, A. *J. Am. Chem. Soc.* **1992**, *114*, 3656.

(97) Turro, C.; Chang, C. K.; Leroi, G. E.; Cukier, R. I.; Nocera, D. G. *J. Am. Chem. Soc.* **1992**, *114*, 4013.

(98) Ho, P. S. *DNA-mediated Electron Transfer and Application to 'Biochip' Development*; Gov. Rep. Announce. Index (U.S.) 1991, 91(23), Abstr. No. 165,497; Report, Order No. AD-A239093, 6 pp. Avail. NTIS, 1991.

Acknowledgment. This work was supported at Georgia State University by a grant to TLN from the United States Department of Energy, Office of Health and Environment, Radiological and Chemical Physics Research Division (Grant No. DE-FG05-03ER61604). T.L.N. acknowledges helpful conversations with Drs. Nicholas Geacintov, Alex Siemiarczuk, and Michael Wasielewski.

Supporting Information Available: The equations in the One to Four Exponentials program used to analyze the emission decay data and figures showing relative emission intensity versus time plots of the normalized lamp emission profile, emission decay, and the instrument-response convoluted fit to the emission decay data and residuals (13 pages). The material is contained in many libraries on microfiche, immediately follows this article in the microfilm version of the journal, can be ordered from the ACS, and can be downloaded from the Internet; see any current masthead page for ordering information and Internet access instructions.

JA950231J